

Second Law Analysis of Diffusion Flames

Dorin STANCIU[#], Dragos ISVORANU, Mircea MARINESCU
Dept. of Engineering Thermodynamics, Polytechnic University of Bucharest
Splaiul Independentei, 313, Bucharest-Romania
Tel: +410 01 3140097, Fax: +410 11 17
E-mail: sdorin@mdd.combustion.pub.ro

Yalcin GOGUS
Middle East Technical University, Aeronautical Eng. Dept.,
Ankara, 06531-Turkey
Fax: +90 312 210 1272
E-mail: ygogus@metu.edu.tr

Abstract

The objective of this paper is to investigate the sources of volumetric irreversibilities in both laminar and turbulent diffusion flames. The theoretical background of analysis relies on the local exergy transport equation, which allows the microscopic formulation of the well-known Gouy-Stodola theorem. For laminar reacting flows, the volumetric entropy generation rate expression includes the viscous, thermal, diffusion and chemical components. Their expressions show that the corresponding irreversibilities are uncoupled if the combustion process occurs at constant pressure. The numerical simulation of a methane-air combustion process shows that the thermal, chemical and diffusive irreversibilities represent, in order of enumeration, the predominant irreversibilities in the laminar diffusion reacting flows. In the case of turbulent diffusion flames, the viscous, thermal, diffusion and chemical mean components have to be expressed in accordance with the combustion model. Two combustion models are used: the multi-species approach based on the eddy-break formulation of mean reaction rate, and the assumed probability density function for a conserved scalar that relies on the flame sheet model. For a diffusion methane-air jet flame, the distribution of mean irreversibility components is presented. Taking into account the technical importance of diffusion flames, the analysis could serve to improve the combustion geometry and the flow condition.

Key words: Reacting flows, entropy generation, diffusion flames, combustion methane-air

1. Introduction

In the field of power generation, the chemically reactive flows have a significant relevance. The flame sheet is the place where the chemical fuel exergy is transferred to thermal exergy of the fluid in an irreversible manner so that a fraction of the exergy is always destroyed.

At the bulk level analysis, the well-known Gouy-Stodola theorem establishes the liaison between the lost exergy and the generation of

entropy. This method can be easily applied, but it hasn't enough accuracy and it doesn't emphasize the peculiarities of the exergy dissipation. Because of the great complexity of the chemical, mass and heat interactions, the continuum level represents the only reasonable approach in the second law analysis of a reacting flow. This level of analysis was first formulated by Bejan (1983), who applied it in the case of laminar single-component flows. It was also used for the single-component turbulent flows (Sciuba, 1994),

[#] Author to whom all correspondence should be addressed.

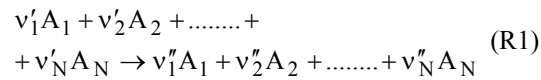
(Stanciu et al., 2000*) where specific dissipation mechanisms are generated by the fluctuating field (Stanciu et al., 2000). In this paper, we extend this method to both laminar and turbulent diffusion flames.

2. Second Law Analysis of Laminar Diffusion Flames

The first step in performing the second law analysis is to obtain the mathematical model of laminar reacting flow. Based on it, the local exergy balance equation will be derived. This equation establishes the liaison between the volumetric entropy generation rate and the local dissipation of the flow exergy. In the following step, the general expression of the volumetric entropy generation rate will be put in an applicable form. Finally, the importance of each irreversibility mechanism on the exergy losses will be numerically investigated in the case of a diffusion methane-air jet flame.

2.1 The mathematical model of diffusion reacting flow

Let us consider a laminar chemically reacting flow of a multi-component gaseous mixture. For the sake of simplicity the flow chemistry is described by a single step reaction:



where v'_i , v''_i represent the stoichiometric coefficients of reactants and products and A_i stands for the chemical species. The mathematical model of the flow consists in the continuity (1), species (2), momentum (3) and energy Eqs. (4a). Their conservative forms are (Libby and Williams, 1993):

$$\frac{\partial \rho}{\partial \tau} + \frac{\partial (\rho u_\alpha)}{\partial x_\alpha} = 0 \quad (1)$$

$$\frac{\partial}{\partial \tau} (\rho Y_i) + \frac{\partial}{\partial x_\alpha} [\rho u_\alpha Y_i + \rho_i \vartheta_\alpha^{(i)}] = (v''_i - v'_i) M_i \rho \omega \quad (2)$$

$i=1, N$

$$\frac{\partial}{\partial \tau} (\rho u_\beta) + \frac{\partial}{\partial x_\alpha} [\rho u_\alpha u_\beta + P \delta_{\alpha\beta} - \tau_{\beta\alpha}^{(V)}] = 0 \quad (3)$$

$\beta=1, 3$

$$\frac{\partial}{\partial \tau} (\rho e^*) + \frac{\partial}{\partial x_\alpha} \left[\rho u_\alpha h^* + \sum_{i=1}^N \rho_i \vartheta_\alpha^{(i)} h_i + \dot{q}_\alpha - \tau_{\alpha\beta}^{(V)} u_\beta \right] = 0 \quad (4a)$$

Of course the total energy e^* and the total enthalpy h^* appearing in the energy Eq. (4a)

both include the energy of formation of the species involved, the kinetic energy and the potential energy of the flow. This equation, which represents the general volumetric formulation of first law of thermodynamics for multi-component systems, can take various forms. In low speed flows, it is customary to adopt the static enthalpy as the variable characterizing the energy content of the fluid, so that Eq. (4a) is replaced by:

$$\frac{\partial}{\partial \tau} (\rho h) + \frac{\partial}{\partial x_\alpha} \left[\rho u_\alpha h + \sum_{i=1}^N \rho_i \vartheta_\alpha^{(i)} h_i + \dot{q}_\alpha \right] = \frac{\partial P}{\partial \tau} \quad (4b)$$

Eqs. (1)-(4) must be completed with the definitions of diffusion velocity $\vartheta_\alpha^{(i)}$, heat flux \dot{q}_α , and viscous stress tensor $\tau_{\beta\alpha}^{(V)}$. With some classical assumptions involving the diffusion phenomena and the absence of radiation, Fick's law, Fourier's law and the Newtonian mixture hypothesis lead to:

$$\rho_i \vartheta_\alpha^{(i)} = -\rho D_{im} \frac{\partial Y_i}{\partial x_\alpha} \quad (5)$$

$$\dot{q}_\alpha = -\lambda_v \frac{\partial T}{\partial x_\alpha} \quad (6)$$

$$\tau_{\alpha\beta}^{(V)} = \mu_v \left[\left(\frac{\partial u_\alpha}{\partial x_\beta} + \frac{\partial u_\beta}{\partial x_\alpha} \right) - \frac{2}{3} \delta_{\alpha\beta} \frac{\partial u_\gamma}{\partial x_\gamma} \right] \quad (7)$$

where μ_v is the molecular viscosity, λ_v represents the thermal conductivity and D_{im} stands for the diffusion coefficient of i -chemical component in mixture. In order to close the system (1) - (4) the equations of state must be added. In these conditions we restrict our analysis to an ideal gas mixture for which:

$$P = \rho R_M T \sum_{i=1}^N \frac{Y_i}{M_i} \quad (8)$$

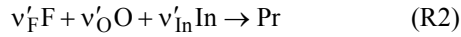
$$h^* = \sum_{i=1}^N Y_i \left(h_i^{(o)} + h_i^{(s)} \right) + \frac{1}{2} u_\alpha u_\alpha = \sum_{i=1}^N Y_i \left(h_i^{(o)} + \int_{T_0}^T c_{p,i} dT \right) + \frac{1}{2} u_\alpha u_\alpha \quad (9)$$

where $h_i^{(o)}$ represents the energy of formation of i -specie and R_M is the universal gas constant. Although the ideal gases mixture hypothesis restrains the generality of the analysis, its important role in the technical combustion processes is well - known.

In this formulation, the mathematical model of reacting flows includes all the chemical

components of gaseous mixture. For this reason, it will be named the multi-species model. It is valid for both diffusion and premixed flames but has the disadvantage of using N+4 equations, which may be expensive from the computational point of view.

In the case of diffusion flames, the number of equations can be dramatically reduced using the Shvab-Zel'dovich approximation that allows the definition of mixture fraction ξ . For a single irreversible reaction that reads:



involving the fuel F, the oxidizer O and the inert specie In as reactants and the products Pr, the mixture fraction is defined as:

$$\xi = \frac{\beta - \beta_1}{\beta_2 - \beta_1} \quad (10)$$

where β is the coupling function and the subscripts 1 and 2 identify the fuel and the oxidizer streams of the two feed system. Assuming a single diffusion coefficient and a Lewis number equal to unity for all chemical components (meaning $D=D_{im}=\text{const.}$ and $Le_i=1$), the species and the energy equations take the same form, so they can be replaced with that of mixture fraction:

$$\frac{\partial(\rho\xi)}{\partial\tau} + \frac{\partial}{\partial x_\alpha} \left(\rho u_\alpha \xi + \rho D \frac{\partial\xi}{\partial x_\alpha} \right) = 0 \quad (11)$$

Finally, in the Burke-Schumann approximation (Burke and Schumann, 1928), all the thermochemical variables can be recovered from the mixture fraction solution:

$$Y_F(\xi) = Y_{F,2} \left(\frac{\xi - \xi_{st}}{1 - \xi_{st}} \right) H(\xi - \xi_{st})$$

$$Y_O(\xi) = Y_{O,1} \left(\frac{\xi_{st} - \xi}{\xi_{st}} \right) [1 - H(\xi - \xi_{st})] \quad (12a,b)$$

$$Y_{in}(\xi) = Y_{in,1} + (Y_{in,2} - Y_{in,1}) \xi$$

$$Y_{pr}(\xi) = 1 - Y_F(\xi) - Y_O(\xi) - Y_{in}(\xi) \quad (12c,d)$$

$$T(\xi) = \begin{cases} T_f(\xi) + \frac{H_F}{M_O v'_O c_p(\xi)} Y_{O,1} (1 - \xi) & \text{for } \xi \geq \xi_{st} \\ T_f(\xi) + \frac{H_F}{M_F v'_F c_p(\xi)} Y_{F,2} \xi & \text{for } \xi \leq \xi_{st} \end{cases} \quad (13)$$

where ξ_{st} is the stoichiometric value of the mixture fraction, and T_f represents the frozen mixture temperature that read:

$$\xi_{st} = \frac{Y_{O,1}}{\frac{v'_O M_O}{v'_F M_F} Y_{F,2} + Y_{O,1}} \quad (14)$$

$$T_f(\xi) = \frac{c_{p,O}}{c_p} T_1 + \left(\frac{c_{p,F}}{c_p} T_2 - \frac{c_{p,O}}{c_p} T_1 \right) \xi \quad (15)$$

In the above expressions, M represents the atomic mass, H_F stands for the lower heating value of fuel and $H(x)$ is the Heaviside step function. Subscripts F, O, in and pr denote the fuel, the oxidizer, the inert and the product species of chemical global reaction (R2) and subscripts 1 and 2 identify the streams of the two feed system. Of course, this model involves some approximations that alter its accuracy, but has the great advantage of solving only four partial differential equations.

2.2 The exergy balance equation

A bulk level analysis shows that reaction (R1) performs the conversion of chemical exergy into a thermal one. Of course, the Gouy-Stodola theorem establishes the liaison between the lost exergy and the conversion irreversibilities. Because of the high complexity of the processes occurring in the chemically reactive mixtures, the bulk level exergy analysis cannot emphasize the peculiarities of the lost exergy mechanisms. So the goal of this paragraph is to derive a local balance equation modeling the transport and the conversion of the exergy.

For a multi-component system, the balance equation of the entropy can be written as:

$$\frac{\partial(\rho s)}{\partial\tau} + \frac{\partial}{\partial x_\alpha} \left[\rho u_\alpha s + \sum_{i=1}^N \rho_i g_\alpha^{(i)} s_i + \dot{q}_\alpha / T \right] = \dot{S}_{gen}^{(\Omega)} \quad (16)$$

The above relation is multiplied with reference temperature which is taken equal to the environment temperature T_0 and the result is subtracted from the total energy Eq. (4a). In order to emphasize the influence of the chemical reaction on the exergy transport mechanism, the enthalpy, entropy and internal energy of the gaseous mixture are split into their reference ^(o) and difference ^(s) parts:

$$h = h^{(o)} + h^{(s)}; \quad e = e^{(o)} + e^{(s)};$$

$$s = s^{(o)} + s^{(s)} \quad (17)$$

The same decomposition is used for the mixture's components. By the ideal gas assumption the reference entropy $s^{(o)}(T_0, P_0)$ can be expressed as:

$$s^{(o)}(T_0, P_0) = \sum_{i=1}^n \left[s_i^{(o)}(T_0, P_0) + R_i \ln X_i \right] \quad (18)$$

where P_0 represents the reference pressure, X_i is the mole fraction of considered specie and $s_i^{(o)}$ entropy of pure specie at P_0 , T_0 . Using the above decompositions and some algebraic transformations, the exergy transport equation reads (Stanciu et al., 2000):

$$\frac{\partial}{\partial \tau} [\rho(\text{ex})] + \frac{\partial}{\partial x_\alpha} \left[\rho u_\alpha (\text{ex}_{h^*}) + \sum_{i=1}^N \rho_i \vartheta_\alpha^{(i)} (\text{ex}_h)_i \right] + (\text{Ex}_Q)_\alpha + (\text{Ex}_\tau)_\alpha = \Pi(\text{ex}) - \Delta(\text{ex}) \quad (19)$$

Eq. (19) is written in the general form of a scalar conservation law. It shows that the variation of the exergy in each point of the flow is due to the convection and diffusion fluxes of exergy and to the exergy source term. The components of the convection flux, which is performed by the transport of exergy with the flow velocity, are:

$$F_\alpha^{(c)}(\text{ex}) = \rho u_\alpha (\text{ex}_{h^*}) = \rho u_\alpha \left[h^* - h^{(o)} - T_0 (s - s^{(o)}) \right] \quad (20)$$

The exergy diffusion flux appears because of the mass, heat and work interactions. Its components can be expressed as:

$$F_\alpha^{(d)}(\text{ex}) = \sum_{i=1}^N \rho_i \vartheta_\alpha^{(i)} (\text{ex}_h)_i + (\text{Ex}_Q)_\alpha + (\text{Ex}_\tau)_\alpha = -\rho \sum_{i=1}^N D_{im} \frac{\partial Y_i}{\partial x_\alpha} \left[h_i - h_i^{(o)} - T_0 (s_i - s_i^{(o)}) \right] - \lambda \frac{\partial T}{\partial x_\alpha} \left(1 - \frac{T_0}{T} \right) - \tau_{\alpha\beta} u_\beta \quad (21)$$

Finally, the exergy source contains both the volumetric production and the volumetric dissipation rates. The volumetric rate of chemical to physical exergy conversion:

$$\Pi(\text{ex}) = -\left\{ \Delta G^{(o)} + R_M T \ln [K_p(T_0)] \right\} \omega > 0 \quad (22)$$

is proportional to the chemical exergy of the reactants, $\zeta_{ch} = -\{ \Delta G^{(o)} + R_M T \ln [K_p(T_0)] \}$, which is released at a rate equal to the chemical reaction rate, ω . But more important for our goal is the volumetric rate of exergy dissipation, which has the expression:

$$\Delta(\text{ex}) = T_0 \dot{S}_{gen}^{(\Omega)} > 0 \quad (23)$$

showing that it is proportional to the volumetric entropy generation rate. Of course the relation (23) represents the local formulation of the Gouy-Stodola theorem.

2.3 The entropy generation rate expression

Eq. (19) shows that at each point of the flow, the exergy variation depends strongly on

the balance between the rate of chemical exergy release, which increases the flow physical exergy and the rate of volumetric entropy generation, which destroys it. We focus at this time on the volumetric entropy generation rate that, in the most general case, can be expressed as (Vilcu, 1988):

$$\dot{S}_{gen}^{(\Omega)} = \frac{\tau_{\beta\alpha}^{(V)}}{T} \frac{\partial u_\beta}{\partial x_\alpha} + \frac{\lambda}{T^2} \frac{\partial T}{\partial x_\alpha} \frac{\partial T}{\partial x_\alpha} - \frac{1}{T} \sum_{i=1}^N \rho_i \vartheta_\alpha^{(i)} \left(\frac{\partial \mu_i}{\partial x_\alpha} \right)_T + \frac{A\omega}{T} \quad (24)$$

where μ_i is the chemical potential of the i -component and A represents the mixture's affinity. In the case of an ideal gas mixture, the chemical potential relation is (Bejan, 1988):

$$\mu_i(T, p, X_i) = \mu_i^{(X_i=1)}(T, p) + R_i T \ln X_i = g_i(T, p) + R_i T \ln X_i \quad (25)$$

where g_i is the specific free enthalpy of the i -component. In this case, the derivatives $(\partial \mu_i / \partial x_\alpha)_T$ can be easily calculated and the expression of the volumetric entropy generation rate (24) becomes (Stanciu et al., 2000):

$$\dot{S}_{gen}^{(\Omega)} = \left(\dot{S}_{gen}^{(\Omega)} \right)_V + \left(\dot{S}_{gen}^{(\Omega)} \right)_Q + \left(\dot{S}_{gen}^{(\Omega)} \right)_D + \left(\dot{S}_{gen}^{(\Omega)} \right)_{CH} \quad (26)$$

The first term of the above relation:

$$\left(\dot{S}_{gen}^{(\Omega)} \right)_V = \frac{\tau_{\beta\alpha}^{(V)}}{T} \frac{\partial u_\beta}{\partial x_\alpha} > 0 \quad (27)$$

represents the viscous part of the volumetric entropy generation rate. It models the flow irreversibilities due to the shear stress tensor. The following two terms:

$$\left(\dot{S}_{gen}^{(\Omega)} \right)_Q + \left(\dot{S}_{gen}^{(\Omega)} \right)_D = \frac{\lambda}{T^2} \frac{\partial T}{\partial x_\alpha} \frac{\partial T}{\partial x_\alpha} + \sum_{i=1}^N \rho D_{im} \left[\frac{R_i}{p} \frac{\partial Y_i}{\partial x_\alpha} \frac{\partial p}{\partial x_\alpha} + \frac{R_i}{Y_i} \frac{\partial Y_i}{\partial x_\alpha} \frac{\partial Y_i}{\partial x_\alpha} \right] > 0$$

model the irreversibilities due to the heat and mass transfer interactions. Although the diffusion phenomena due to the pressure and temperature gradients were neglected in Fick's law (5), these irreversibilities are still coupled through the product $(\partial Y_i / \partial x_\alpha \cdot \partial p / \partial x_\alpha)$ which has an unknown sign. But neglecting the diffusion due to the pressure gradients, as in Eq. (5), means that:

$$|dP/P| \ll |dY_i/Y_i|$$

The above hypothesis has a wide validity because many engineering applications of combustion processes happen at $P \approx \text{const}$. In this

case, the thermal and diffusion irreversibilities uncouple so that:

$$\left(\dot{S}_{\text{gen}}^{(\Omega)}\right)_Q = \frac{\lambda}{T^2} \frac{\partial T}{\partial x_\alpha} \frac{\partial T}{\partial x_\alpha} > 0 \quad (28)$$

$$\left(\dot{S}_{\text{gen}}^{(\Omega)}\right)_D = \sum_{i=1}^N \rho D_{im} \frac{R_i}{Y_i} \frac{\partial Y_i}{\partial x_\alpha} \frac{\partial Y_i}{\partial x_\alpha} > 0 \quad (29)$$

Finally, the last term in the expression of the volumetric entropy generation rate:

$$\left(\dot{S}_{\text{gen}}^{(\Omega)}\right)_{CH} = \frac{A\omega}{T} = \frac{\omega}{T} \sum_{i=1}^N (v_i' - v_i'') \mu_{M,i} > 0 \quad (30)$$

model the chemical irreversibilities due to reaction (R1). It can be seen that this term depends on the chemical reaction rate, and the molar chemical potential $\mu_{M,i}$ of each species.

2.4 Numerical simulation of laminar diffusion flame irreversibilities

As an application of the above relations, let us consider the coaxial jet diffusion flame of methane-air laminar combustion. Burner geometry and boundary conditions are presented in *Figure 1*. The fuel, having the inlet velocity of 0.5 m/s, enters into the burner through a circular inlet with diameter $d=2$ mm and the surrounding air meets the methane jet with an inlet velocity of 0.05 m/s. The two coaxial jets are bounded by an adiabatic outer wall.

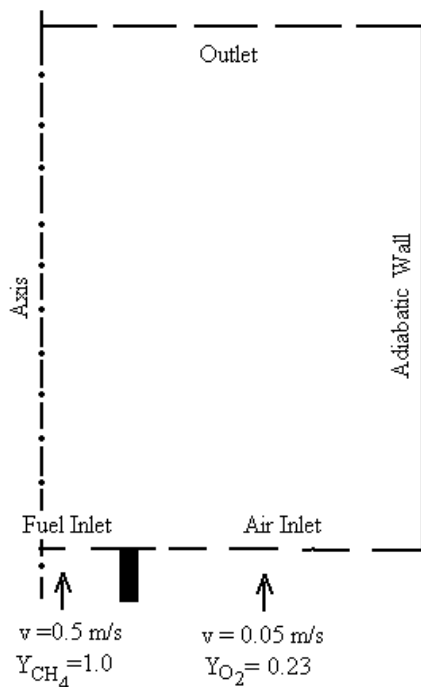


Figure 1. Burner geometry and boundary conditions for laminar flame calculation

The flame chemistry is modeled by a single step chemical reaction like (R1) and the reacting flow is governed by Eq. (1-4b). The numerical calculation was performed with the computer code FLUENT 5.1.

Distribution of the viscous part of volumetric entropy generation rate has very small values so it wasn't plotted. Of course the highest dissipation rates take place near burner entrance region because of the inlet velocity difference between the two coaxial jets. A viscous dissipation of the same magnitude also occurs around the adiabatic wall of the burner where the non-slip boundary condition generates high velocity gradients.

Figure 2a presents the distribution of the thermal component of volumetric entropy generation rate. By far this kind of dissipation is more important than the viscous one. The extremely high temperature gradients in the flame front proximity generate the maximal thermal dissipation in this area. Another place of significant thermal dissipation is located around the fuel entrance because of the heat transfer from the flame. As expected, the maximal values of thermal irreversibilities decrease along the front of the flame due to the cutting down of temperature gradients. The diffusion component variation of the volumetric entropy generation rate is presented in *Figure 2b*. As in previous cases the most important diffusion dissipations are located around the flame front, but their values are smaller than in the previous case. *Figure 2c* shows the distribution of chemical volumetric entropy generation rate. The highest values of this irreversibility component are found in the flame front where the most important part of the chemical transformations happens. It can also be seen that in the sites where they take place, the chemical irreversibilities remain the most significant among the flow irreversibilities.

The distribution of the total volumetric entropy generation rate is presented in *Figure 3*. It is easy to point out that around the flame front, this distribution is identical with that of the chemical volumetric rate, which rules in this area. Along the normal direction at the front of the flame, the methane's concentration continuously decreases and the reaction rate slows down. As a consequence, the chemical dissipation becomes smaller and smaller so that, in these sites, the shape of the volumetric entropy generation rate is formed by the thermal component of the irreversibilities. It is surprising that the diffusion part of volumetric dissipations, that are greater than in the case of premixed flame (Stanciu et al., 2000), doesn't seriously affect the shape of irreversibility distribution.

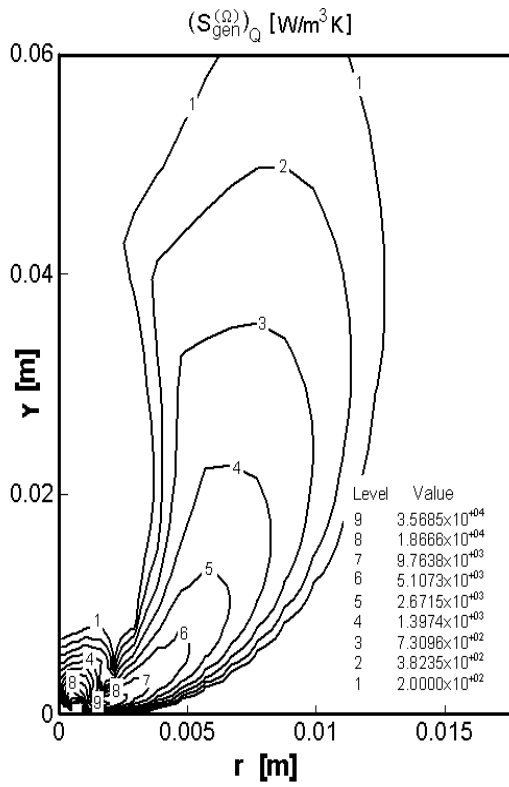


Figure 2a. Thermal irreversibility component

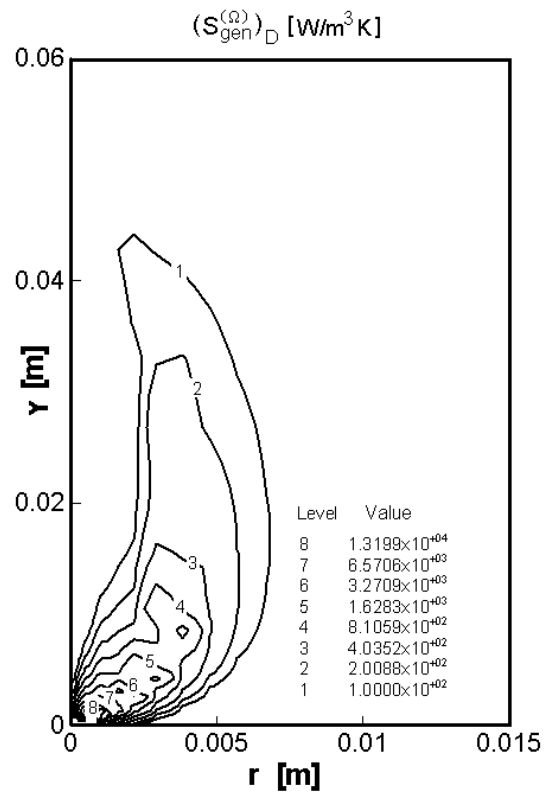


Figure 2b. Diffusion irreversibility component

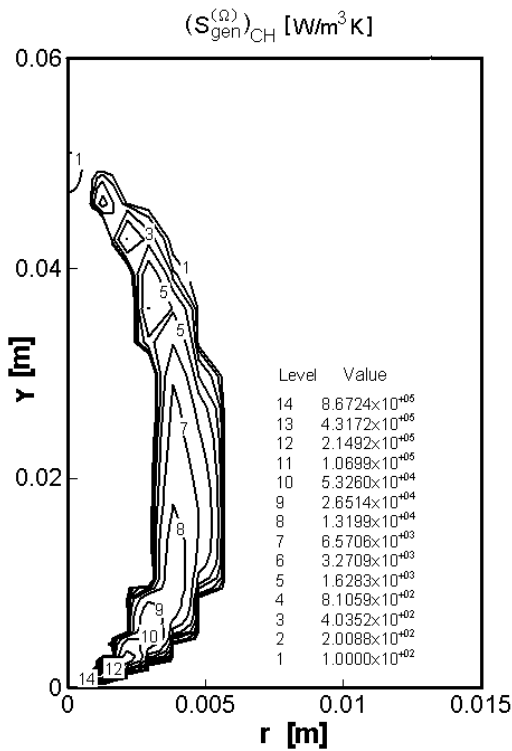


Figure 2c. Chemical irreversibility component

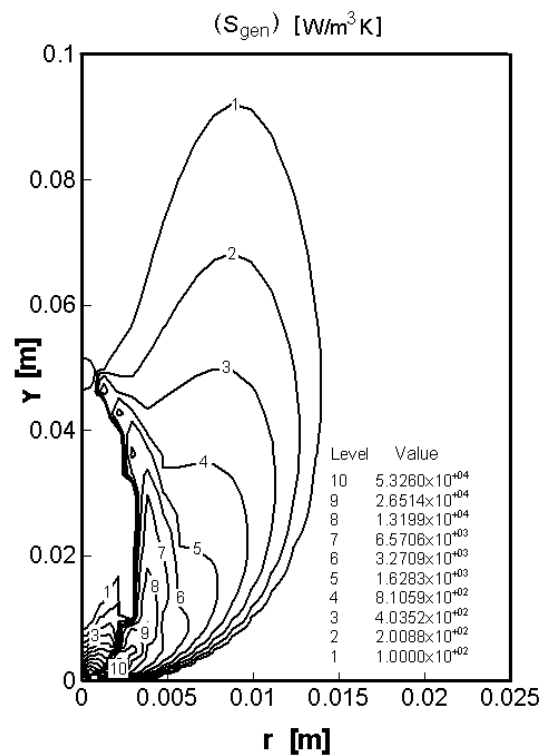


Figure 3. Computed distribution of volumetric irreversibility for a laminar diffusion flame

TABLE I. INTEGRAL VALUES OF ENTROPY GENERATION RATES AND ENTROPY FLUX FOR LAMINAR FLAME

$\left(\dot{\bar{S}}_{gen}\right)_V$	$\left(\dot{\bar{S}}_{gen}\right)_Q$	$\left(\dot{\bar{S}}_{gen}\right)_D$	$\left(\dot{\bar{S}}_{gen}\right)_{CH}$	$\dot{\bar{S}}_{gen}$	Entropy flux	Error
[W/K]	[W/K]	[W/K]	[W/K]	[W/K]	[W/K]	[%]
1.3×10^{-9}	0.02477	0.00266	0.0197	0.04713	0.04672	0.87

For the sake of clarity, the smallest values of volumetric entropy generation rate were removed from *Figures 2* and *3*.

Reacting flow irreversibility model, as well as the precision of calculation can be verified with the aid of the entropy transport Eq. (16). Taking into account that vertical boundaries are adiabatic and the outlet boundary is far from the flame front, the integral of this equation reduces to:

$$\iint_{\partial\Omega_C} \rho \tilde{u} \cdot \tilde{n} d\Sigma = \iiint_{\Omega_C} \dot{\bar{S}}_{gen}^{(\Omega)} d\Omega \quad (31)$$

where $\partial\Omega_C$ denotes the boundaries of computational domain Ω . The values of the entropy generation rate components on Ω and the entropy flux value through $\partial\Omega$ are presented in TABLE I. It can be seen that the error between the two sides of the above equation is less than 0.9%, but more important than that, the thermal and chemical irreversibilities are responsible for about 95% of the laminar flame dissipations.

3. Second Law Analysis of Turbulent Diffusion Flames

Although the turbulent combustion is by far more complex than the laminar one, the requested steps in deriving its second law analysis are the same. The differences come out from the turbulence and combustion closure models that strongly influence the averaging methodology of volumetric entropy generation rate expression.

3.1 The mathematical model of turbulent reacting flow

There are many ways in modeling the turbulent reacting flows of diffusion flames. All of them are based on the time average of Eqs. (1)-(4b) at which a turbulence closure model and a combustion closure model must be added. The difference among the models consists in the computation of the averaged thermochemical flow variables as \tilde{Y}_i , \tilde{h} and $\tilde{\omega}$. In this paper we used two distinct models: the multi-species approach, and the assumed probability density function for a conserved scalar.

3.1.1 The multi-species model

This model uses the average of full reacting flow equations. At this moment it is widely accepted that Favre decomposition of all instantaneous properties, except density and pressure, provides the most convenient way for obtaining the averaged continuity (32), species (33), momentum (34) and enthalpy (35) equations which become:

$$\frac{\partial \bar{\rho}}{\partial \tau} + \frac{\partial (\bar{\rho} \tilde{u}_\alpha)}{\partial x_\alpha} = 0 \quad (32)$$

$$\begin{aligned} \frac{\partial}{\partial \tau} (\bar{\rho} \tilde{Y}_i) + \frac{\partial}{\partial x_\alpha} \left[\bar{\rho} \tilde{u}_\alpha \tilde{Y}_i - \overline{\Phi_{i,\alpha}^{(V)}} + \overline{\Phi_{i,\alpha}^{(R)}} \right] = \\ = (v_i'' - v_i') M_i \bar{\rho} \tilde{\omega} \end{aligned} \quad (33)$$

$i=1,N$

$$\frac{\partial}{\partial \tau} (\bar{\rho} \tilde{u}_\beta) + \frac{\partial}{\partial x_\alpha} \left[\bar{\rho} \tilde{u}_\alpha \tilde{u}_\beta + \bar{P} \delta_{\alpha\beta} - \overline{\tau_{\beta\alpha}^{(V)}} + \overline{\tau_{\beta\alpha}^{(R)}} \right] = 0 \quad (34)$$

$\beta=1,3$

$$\frac{\partial}{\partial \tau} (\bar{\rho} \tilde{h}) + \frac{\partial}{\partial x_\alpha} \left[\bar{\rho} \tilde{u}_\alpha \tilde{h} - \overline{\dot{q}_\alpha^{(V)}} + \overline{\dot{q}_\alpha^{(R)}} \right] = \frac{\partial \bar{P}}{\partial \tau} \quad (35)$$

For the sake of simplicity, in Eq. (35) we used the assumption $Le=1$. In the above equations:

$$\overline{\Phi_{i,\alpha}^{(V)}} = -\bar{\rho} D_{im} \frac{\partial \tilde{Y}_i}{\partial x_\alpha} \quad (36)$$

$$\overline{\tau_{\beta\alpha}^{(V)}} = \mu_V \left(\frac{\partial \tilde{u}_\alpha}{\partial x_\beta} + \frac{\partial \tilde{u}_\beta}{\partial x_\alpha} \right) - \frac{2}{3} \delta_{\alpha\beta} \frac{\partial \tilde{u}_\gamma}{\partial x_\gamma} \quad (37)$$

$$\overline{\dot{q}_\alpha^{(V)}} = \frac{\mu_V}{Pr} \frac{\partial \tilde{h}}{\partial x_\alpha} \quad (38)$$

denote the mass diffusion mean vector, the viscous mean stress tensor and the mean heat flux vector, while:

$$\begin{aligned} \overline{\Phi_{i,\alpha}^{(R)}} &= -\overline{\rho u_\alpha'' Y_i''} & \overline{\tau_{\beta\alpha}^{(R)}} &= -\overline{\rho u_\alpha'' u_\beta''} \\ \overline{\dot{q}_\alpha^{(R)}} &= -\overline{\rho u_\alpha'' h''} \end{aligned} \quad (39a,b,c)$$

represent the corresponding Reynolds quantities. In order to solve the system (32)-(35), a closure turbulence model for expressions (39) and a combustion model for the mean reaction rate $\tilde{\omega}$ must be added.

Although it has been widely criticized, the turbulence closure model based on gradient transport techniques is very practical for engineering calculation. This model relies on the Boussiesq hypothesis, which connects the Reynolds stress tensor $\tau_{\beta\alpha}^{(R)}$ and the mean strain rate tensor through the turbulent viscosity μ_T . Most often it is computed using the Prandtl-Kolmogorov relation, accomplished by the two equations K- ϵ_K turbulence model, with a wall function treatment of the near wall region. It is well-known that the model fails in predicting the separated and swirling flows or the spreading rate of round jet, which are most often used in combustion processes. In order to improve its behavior, some corrections on ϵ equation, or some modifications of model constants C_μ , C_{ϵ_1} and C_{ϵ_2} must be added, but they depend on the flow type. Another option is to use an improved formulation, like the RNG K- ϵ_K model (Fluent Inc.), which enhances the prediction accuracy of swirling flows, or the Realizable K- ϵ model of Shih (Shih et al., 1995) that clearly improves the spreading rate simulation of both planar and round jets. Using the same gradient transport model closure, the Reynolds mass diffusion vector $\overline{\Phi}_{1,\alpha}^{(R)}$ is related to the mean mass fraction gradient through the turbulent diffusion coefficient D_T , and the Reynolds heat flux vector $\overline{q}_\alpha^{(R)}$ is connected to the mean enthalpy gradient using the turbulent heat transfer coefficient λ_T . These turbulent quantities are computed with the aid of turbulent Schmidt and Prandtl numbers. For standard and realizable K- ϵ_K models, these turbulent quantities are constant, (i.e. $Sc_T=0.7$ and $Pr_T=0.85$), while for RNG K- ϵ_K model they vary following an algebraic relation.

In the case of diffusion flames, the characteristic chemical kinetics time is much smaller than the turbulent mixing time so that the mixing always controls the combustion rate. The eddy break-up models are mixing controlled combustion techniques that determine the mean reaction rate $\tilde{\omega}$ as a function of mean mass fraction field, \tilde{Y}_i and the characteristic time of turbulence, K/ϵ . For this work we selected the well-known eddy-break formulation of Magnussen and Hjertager (Magnussen and Hjertager, 1976).

3.1.2 Assumed probability density function model for a conserved scalar

The above model has the great disadvantage of involving all the flow and thermo-chemical variables. In these conditions it needs a lot of computational time, especially for complex flow geometry that often requests a fine discretization. At the opposite extremity is placed the assumed probability density function (PDF) approach for a conserved scalar. This model relies only on the averaged continuity (32) and momentum (34) equations at which a turbulence closure model must be added. For this paper we used the standard K- ϵ_K turbulence model, adapted for the round jet calculation with Launder's correction (Launder et al., 1972). All the mean thermo-chemical properties, including here the averaged mass fractions and the mean temperature, are computed with the relation:

$$\tilde{\phi} = \int_0^1 \phi(\xi) \tilde{f}(\xi) d\xi \quad (40)$$

where $\phi(\xi)$ is a generic instantaneous flow variable whose solution results from the Burke-Schumann approximations (12)-(13) and $\tilde{f}(\xi)$ is the PDF of the mixture fraction. Assuming for PDF a clipped Gaussian distribution:

$$\tilde{f}(\xi) = \alpha_0 \delta(\xi) + \alpha_1 \delta(\xi-1) + \frac{1}{\sigma\sqrt{2\pi}} \exp\left[-\frac{1}{2}\left(\frac{\xi-\mu}{\sigma}\right)^2\right] [H(\xi) - H(\xi-1)] \quad (41)$$

the local parameters σ , μ , α_0 and α_1 are determined functions of mean mixture fraction and mixture fraction variance (Elghobashi, 1977), (Lockwood, 1977) for which the corresponding averaged transport equations are added.

3.2 The mathematical model of turbulent reacting flow irreversibilities

The first step in modeling the flow irreversibilities is to average the instantaneous entropy Eq. (16) which leads to:

$$\frac{\partial(\overline{\rho s})}{\partial \tau} + \frac{\partial}{\partial x_\alpha} \left[\overline{\rho u_\alpha s} + \overline{\rho u_\alpha'' s''} - \sum_{i=1}^N \overline{\rho D_{im}} \frac{\partial \tilde{Y}_i}{\partial x_\alpha} \tilde{s}_i - \sum_{i=1}^N \overline{\rho D_{im}} \frac{\partial Y_i''}{\partial x_\alpha} s_i'' + \overline{q}/T \right] = \dot{S}_{gen}^{(\Omega)} \quad (42)$$

It is not very easy to model the correlations appearing on the left hand side of the above equation. But as in the laminar case, with some simplifications imposed by the boundary conditions, it can be used for checking the

veridicality of irreversibility model as well as the accuracy of numerical calculations.

The averaged form of the instantaneous exergy Eq. (19) is not presented here because it is not used in computations. But it leads to the very important conclusion that:

$$\Delta[\overline{\rho(\text{ex})}] = T_0 \dot{\overline{S}}_{\text{gen}}^{(\Omega)} > 0 \quad (43)$$

which constitutes the theoretical basis of second law analysis of turbulent flames. Indeed, the above relation shows that the destroying rate of Favre averaged volumetric exergy is proportional to the Reynolds averaged volumetric rate of entropy generation. In this condition, an accurate determination of mean entropy generation rate, $\dot{\overline{S}}_{\text{gen}}^{(\Omega)}$ becomes crucial for both the second law analysis of turbulent reacting flow and the lost exergy computation.

Including the thermo-chemical properties and their gradients, the averaging procedure of volumetric entropy generation rate expression needs to take into account the mathematical model used for reacting flow. In the following sections we present the averaged expression of the volumetric entropy generation rate for both mathematical flow models used in this work.

3.2.1 Averaging the entropy generation rate for the multi-species model

The Reynolds average procedure applied to the instantaneous entropy generation rate expression (26) leads to:

$$\dot{\overline{S}}_{\text{gen}}^{(\Omega)} = \left(\dot{\overline{S}}_{\text{gen}}^{(\Omega)}\right)_V + \left(\dot{\overline{S}}_{\text{gen}}^{(\Omega)}\right)_Q + \left(\dot{\overline{S}}_{\text{gen}}^{(\Omega)}\right)_D + \left(\dot{\overline{S}}_{\text{gen}}^{(\Omega)}\right)_{\text{CH}} \quad (44)$$

In order to find the averaged expressions of volumetric entropy generation rate components (27)-(30), the instantaneous temperature, as well as the instantaneous mass fraction, are decomposed into their mean and fluctuating parts. So using the hypothesis $T''/\tilde{T} \ll 1$, and dropping the serial decomposition of $T^{-1} = \tilde{T}^{-1}(1 + T''/\tilde{T})^{-1}$ at the first term, the following expression for volumetric viscous part of entropy generation rate is obtained:

$$\begin{aligned} \left(\dot{\overline{S}}_{\text{gen}}^{(\Omega)}\right)_V &\cong \left(\dot{\overline{S}}_{\text{gen}}^{(\Omega)}\right)_{\text{VM}} + \left(\dot{\overline{S}}_{\text{gen}}^{(\Omega)}\right)_{\text{VT}} \cong \\ &\cong \frac{\tilde{\tau}_{\beta\alpha}^{(V)}}{\tilde{T}} \frac{\partial \tilde{u}_\beta}{\partial x_\alpha} + \frac{\bar{\rho} \varepsilon_K}{\tilde{T}} \end{aligned} \quad (45)$$

The first term of the above expression models the viscous irreversibilities of mean motion field due to the gradients of averaged velocity. It is the homologue of the term modeling the laminar viscous irreversibilities because it is generated by

the same mechanism. The following term, containing the dissipation rate

$\varepsilon_K = \overline{\tau_{\beta\alpha}^{(V)} (\partial u_\beta'' / \partial x_\alpha) / \bar{\rho}}$ of turbulent kinetic energy $K = \frac{1}{2} \overline{\rho u_\alpha'' u_\alpha''} / \bar{\rho}$ models the proper viscous irreversibilities generated by the flow turbulence. Continuing the averaging procedure and dropping the serial decompositions of $T^{-2} = \tilde{T}^{-2} (1 + T''/\tilde{T})^{-2}$ and $Y_i^{-1} = \tilde{Y}_i^{-1} (1 + Y_i''/\tilde{Y}_i)^{-1}$ at the first term, the following two components of volumetric entropy generation rate (44) can be expressed as:

$$\begin{aligned} \left(\dot{\overline{S}}_{\text{gen}}^{(\Omega)}\right)_Q &= \left(\dot{\overline{S}}_{\text{gen}}^{(\Omega)}\right)_{\text{QM}} + \left(\dot{\overline{S}}_{\text{gen}}^{(\Omega)}\right)_{\text{QT}} \cong \\ &\cong \frac{\lambda_V}{\tilde{T}^2} \frac{\partial \tilde{T}}{\partial x_\alpha} \frac{\partial \tilde{T}}{\partial x_\alpha} + \frac{\bar{\rho} c_p}{\tilde{T}^2} \varepsilon_\theta \end{aligned} \quad (46)$$

$$\begin{aligned} \left(\dot{\overline{S}}_{\text{gen}}^{(\Omega)}\right)_D &= \left(\dot{\overline{S}}_{\text{gen}}^{(\Omega)}\right)_{\text{DM}} + \left(\dot{\overline{S}}_{\text{gen}}^{(\Omega)}\right)_{\text{DT}} \cong \\ &\cong \sum_{i=1}^N \bar{\rho} D_{\text{im}} \frac{R_i}{\tilde{Y}_i} \frac{\partial \tilde{Y}_i}{\partial x_\alpha} \frac{\partial \tilde{Y}_i}{\partial x_\alpha} + \sum_{i=1}^N \frac{R_i}{\tilde{Y}_i} \bar{\rho} \varepsilon_\psi^{(i)} \end{aligned} \quad (47)$$

where:

$$\varepsilon_\theta = (\lambda_V / \bar{\rho} c_p) \overline{\rho (\partial T / \partial x_\alpha) (\partial T'' / \partial x_\alpha) / \bar{\rho}}$$

represents the dissipation rate of fluctuating temperature variance $K_\theta = \frac{1}{2} \overline{\rho T''^2} / \bar{\rho}$ and:

$$\varepsilon_\psi^{(i)} = D_{\text{im}} \overline{(\partial Y_i / \partial x_\alpha) (\partial Y_i'' / \partial x_\alpha)}$$

is the dissipation rate of fluctuating i -component mass fraction variance $K_\psi^{(i)} = \frac{1}{2} \overline{\rho Y_i''^2} / \bar{\rho}$. As in the previous case, the first terms of the right hand side of Eqs. (46) and (47) model the mean motion field irreversibilities, while the second terms take into account the mean dissipations of fluctuating field. For instance, the mean chemical source term is modeled as:

$$\left(\dot{\overline{S}}_{\text{gen}}^{(\Omega)}\right)_{\text{CH}} \cong \frac{\tilde{\omega}}{\tilde{T}} \sum_{i=1}^N (v_i' - v_i'') \tilde{\mu}_{M,i} \quad (48)$$

where the mean chemical potential is simply computed as $\tilde{\mu}_{M,i} = \tilde{h}_{M,i} - \tilde{T} s_{M,i}(\tilde{T}, \bar{p}, \tilde{X}_i)$

Correlating the irreversibility model and the mathematical formulation of diffusive reacting flow, it can be seen that only the mean motion irreversibilities, denoted by subscript M , and the turbulent viscous one, identified by subscript VT can be computed. For both thermal turbulent and diffusion turbulent irreversibilities, the mathematical formulation of reacting flow does not give any information, because its procedures

in computing λ_T and D_T rely on the classical Pr_T and Sc_T determinations, which either are assumed as constants or are computed with some algebraic relations. In this case, the equilibrium turbulence feature can be invoked for which the production and the dissipation terms appearing in K_θ and $K_\psi^{(i)}$ equations are equal. This leads to:

$$\left(\dot{\bar{S}}_{gen}^{(\Omega)}\right)_{QT} = \frac{\bar{\rho}c_p}{\bar{T}^2} \varepsilon_\theta \equiv \frac{\lambda_T}{\bar{T}^2} \frac{\partial \bar{T}}{\partial x_\alpha} \frac{\partial \bar{T}}{\partial x_\alpha} \quad (49)$$

$$\left(\dot{\bar{S}}_{gen}^{(\Omega)}\right)_{DT} = \sum_{i=1}^N \frac{R_i}{\bar{Y}_i} \bar{\rho} \varepsilon_\psi^{(i)} \equiv \bar{\rho} D_T \sum_{i=1}^N \frac{R_i}{\bar{Y}_i} \frac{\partial \bar{Y}_i}{\partial x_\alpha} \frac{\partial \bar{Y}_i}{\partial x_\alpha} \quad (50)$$

The above approximations may be removed if the transport equations of K_θ and $K_\psi^{(i)}$ are added at the mathematical reacting flow model. Then, the dissipation rates appearing in their source terms could be computed as $\varepsilon_\theta = C_\theta (\varepsilon_K / K) K_\theta$ and $\varepsilon_\psi^{(i)} = C_\psi^{(i)} (\varepsilon_K / K) K_\psi^{(i)}$, avoiding the use of additional transport equations for ε_θ and $\varepsilon_\psi^{(i)}$.

Being capable of separating for the first three irreversibility components the mean motion part from the turbulent part, the model reveals almost all the structure of flame dissipations. Even if it may be less accurate in predicting the mean flow properties, this model is useful for studying the influence of turbulence on flame dissipations.

3.2.2 Averaging the entropy generation rate for assumed probability density function model of a conserved scalar

As in the previous case, averaging the instantaneous entropy generation rate expression (26), the relation (44) is recovered. As in the previous case, the viscous component of volumetric entropy generation rate is computed with relation (45), because the mean motion field of the flow has the same model. The differences between the models appear for the following components of volumetric irreversibilities. So, extending the PDF function of conserved scalar (41) to the thermal and diffusion volumetric components of the entropy generation rate, and averaging their instantaneous expressions (28) and (29), it results in (Isvoranu, 1999), (Isvoranu et al., 2000):

$$\left(\dot{\bar{S}}_{gen}^{(\Omega)}\right)_Q = \frac{\bar{\rho}}{2} \tilde{\chi} \int_0^1 \rho c_p \left(\frac{dT}{d\xi}\right)^2 \frac{f(\xi)}{T^2(\xi)} d\xi \quad (51)$$

$$\left(\dot{\bar{S}}_{gen}^{(\Omega)}\right)_D = \frac{\bar{\rho}}{2} \tilde{\chi} \int_0^1 \left[\sum_{i=1}^N \frac{R_i}{\bar{Y}_i} \left(\frac{dY_i}{d\xi}\right)^2 \right] f(\xi) d\xi \quad (52)$$

where $\tilde{\chi}$ is the mean scalar dissipation rate of the mixture fraction, defined as:

$$\tilde{\chi} = \frac{2}{\bar{\rho}} \left[\overline{\rho D \frac{\partial \xi''}{\partial x_\alpha} \frac{\partial \xi''}{\partial x_\alpha}} \right] = 2D \frac{\partial \tilde{\xi}}{\partial x_\alpha} \frac{\partial \tilde{\xi}}{\partial x_\alpha} \quad (53)$$

Based on the Burke-Schumann chemical model (12)-(13), we can now describe all instantaneous mass fractions and instantaneous temperature derivatives as follows:

$$\begin{aligned} \frac{dY_F}{d\xi} &= \begin{cases} \frac{Y_{F,2}}{1-\xi_{st}} & \xi \geq \xi_{st} \\ 0 & \xi < \xi_{st} \end{cases} \\ \frac{dY_O}{d\xi} &= \begin{cases} 0 & \xi \geq \xi_{st} \\ -\frac{Y_{O,1}}{\xi_{st}} & \xi < \xi_{st} \end{cases} \\ \frac{dY_{in}}{d\xi} &= Y_{in,2} - Y_{in,1} \end{aligned} \quad (54a,b,c)$$

$$\frac{dT}{d\xi} = \begin{cases} -T_f - \frac{H_i}{M_O \nu_O c_p} Y_{O,1} & \xi \geq \xi_{st} \\ -T_f + \frac{H_i}{M_F \nu_F c_p} Y_{F,2} & \xi < \xi_{st} \end{cases} \quad (55)$$

Utilizing the conserved scalar model, the chemical component of the volumetric entropy generation rate (30) can be put in the following form (Isvoranu, 1999), (Isvoranu et al., 2000):

$$\left(\dot{\bar{S}}_{gen}^{(\Omega)}\right)_{CH} = \frac{\bar{\rho}}{2} \tilde{\chi} \int_0^1 \left[\frac{1}{T(\xi)} \sum_{i=1}^N \mu_i(\xi) \frac{d^2 Y_i}{d\xi^2} \right] f(\xi) d\xi \quad (56)$$

For a single step irreversible reaction (R2), the second derivatives of the mass fractions appearing in the above relation can be expressed as function of stoichiometric coefficients only, for example, fuel second derivative:

$$\frac{d^2 Y_F}{d\xi^2} = \frac{Y_{F,2}}{(1-\xi_{st})} \delta(\xi - \xi_{st}) \quad (57)$$

where δ represents the Dirac function. Using this relation, the chemical entropy source term (56) becomes:

$$\left(\dot{\bar{S}}_{gen}^{(\Omega)}\right)_{CH} = \frac{\rho_{st}}{2} \tilde{\chi}_{st} \frac{1}{T_{st}} \frac{Y_{F,2}}{1-\xi_{st}} \left(\sum_{i=1}^N \mu_i \nu_i \right) f(\xi_{st}) \quad (58)$$

where the subscript *st* denotes the stoichiometric conditions.

Unfortunately, the expressions (51), (52) and (58) include both the mean motion and the turbulent parts of volumetric irreversibility components because this model doesn't have the

ability to separate them. But the assumed PDF approach gives more realistic results in simulating the reacting flow properties than the multi-species model so it is widely used in diffusion flame simulations. Combining the conclusions revealed by the two models, some important conclusions concerning the irreversibility structure of flame dissipations may be obtained.

3.3 Numerical simulation of turbulent diffusion flame irreversibilities

As an application, let us consider the combustion occurring in a Delft piloted diffusion flame burner that was designed to yield a stable axial-symmetric turbulent non-premixed flame of methane burning in a co-flowing air stream. The fuel jet exit has an inner diameter of 6 mm and the fuel pipe is about 1 m long, sufficient to establish a fully developed turbulent flow at the nozzle. Two air streams are involved. The primary air is issued from an annulus around the fuel nozzle with an inner diameter of 15 mm and an outer diameter of 45 mm. The bulk velocity of the primary air is of 4 m/s while for the methane/nitrogen mixture we have 20 m/s. *Figure 4* shows a cross section through the burner. The annular air is surrounded by a low speed co-flowing air stream of about 0.4 m/s, just sufficient to avoid external recirculation zone. A throat, yielding low turbulence levels at the entrance of the combustion chamber and reasonably flat velocity profile, issues this secondary air, which is kept at room temperature (295 K). The burner is 58 cm in diameter and 150 cm in length to allow major simplifications for boundary conditions and a geometrical point of view, which is axial-symmetric flow and homogenous Neumann outlet conditions.

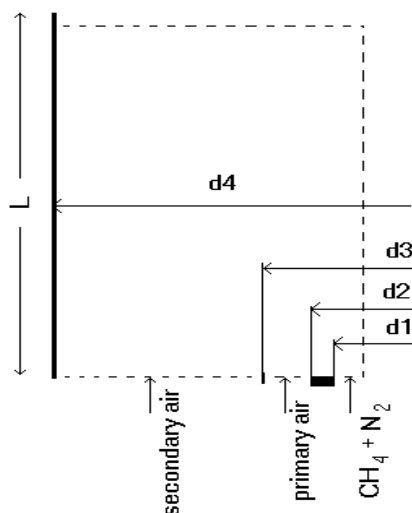


Figure 4. Delft burner geometry (Peeters, 1995)

3.3.1 Flame irreversibility simulation with multi-species model

For multi-species model, the numerical simulation of diffusion flame was performed with the computer code FLUENT 5.1. The flame chemistry was described by a single step irreversible reaction, like (R1) and for turbulence models both RNG K- ϵ and Realizable K- ϵ formulation were selected, which led to similar results. In both cases, the accuracy of the numerical solution was improved by adapting the mapped grid, used for this simulation in accordance with the mean temperature gradient.

The agreement between the numerical solution and the experimental data is acceptable for both turbulence models. For example, at $y=0.05$ m and $y=0.15$ m high from the burner the computed radial temperature distribution is reasonable, but at $y=0.25$ m its simulated distribution exceeds the experimental data with over 200 K. This happens because the spreading rate of fuel jet is over-predicted so that the jet penetration is lower than in the real case. Besides, it cannot be forgotten that eddy-break up models relate the mean reaction rate to the turbulent time scale, which is K/ϵ . It seems that in the middle of the flame this approach leads to higher values of mean reaction rate than the real one.

As previously emphasized, the irreversibility model relying on the multi-species approach is generally capable of distinguishing between the characteristic mean motion dissipations and those induced by turbulence. The distributions of all irreversibility components are presented in *Figure 5*. We note that the thermal turbulent and the diffusion turbulent components were computed with the expressions (49)-(50) and the clarity of representations was improved by removing the smallest values of volumetric entropy generation rate components. In order to compare the influence of fluctuating field on volumetric dissipations, the mean motion and the turbulent parts of viscous, thermal and diffusion irreversibilities are plotted together in the same figure. The common feature of all irreversibility components is that their maximal values occur in the near burner regions and, due to the convection processes, decrease along the front of the flame. On the other hand, it can be seen that the turbulent parts of flame irreversibilities always exceed the corresponding mean motion ones. There are also some peculiar features of each irreversibility component. For example, as shown in *Figure 5a*, the viscous mean motion and viscous turbulent irreversibilities are higher near the burner rim where a small recirculation zone appears. The difference between these

distributions occurs on the fuel side and at the mixing plane where the fuel-oxidizer interactions strongly affect the production and the dissipation of turbulent kinetic energy. The mean motion and turbulent parts of thermal irreversibility, of which distributions are plotted in *Figure 5b*, act in both fuel and oxidizer sides because of the heat transfer, unfolding from the front of the flame to the methane jet and primary air stream. From *Figure 5c* it can be seen that, as in the previous case, the mean and turbulent parts of diffusion irreversibility have similar distributions, but their action takes place in the mixing plane between the expanding fuel jet and the primary air stream. Special attention must be paid for the chemical component of flame irreversibility of which distribution is displayed in *Figure 5d*. Of course, the chemical irreversibilities are concentrated in a thin region bordering the front of the flame, but their higher values lie from the burner rim until the middle of the flame. In this condition the spatial domain

seriously affected by this kind of dissipation is greater than in previous cases.

Now having determined the volumetric components of entropy generation rate, we can proceed to verify both the accuracy of numerical simulation and the veridicality of the irreversibility model. As in the laminar case, this goal can be achieved by checking the closing precision of the entropy transport Eq. (42). Theoretically, this verification may be applied at the local level for each control volume, as well as at global level for the entire flow domain. Due to the complex task of modeling the correlations revealed by Eq. (42), we restrict the verification only at the global level. Taking into account the flow boundary conditions, for the steady state adiabatic systems the entropy Eq. (42) becomes:

$$\int_{\partial\Omega_C} \bar{\rho} \bar{s} \vec{u} \cdot \vec{n} d\Sigma = \int_{\Omega_C} \dot{\bar{S}}_{gen}^{(\Omega)} d\Omega \quad (59)$$

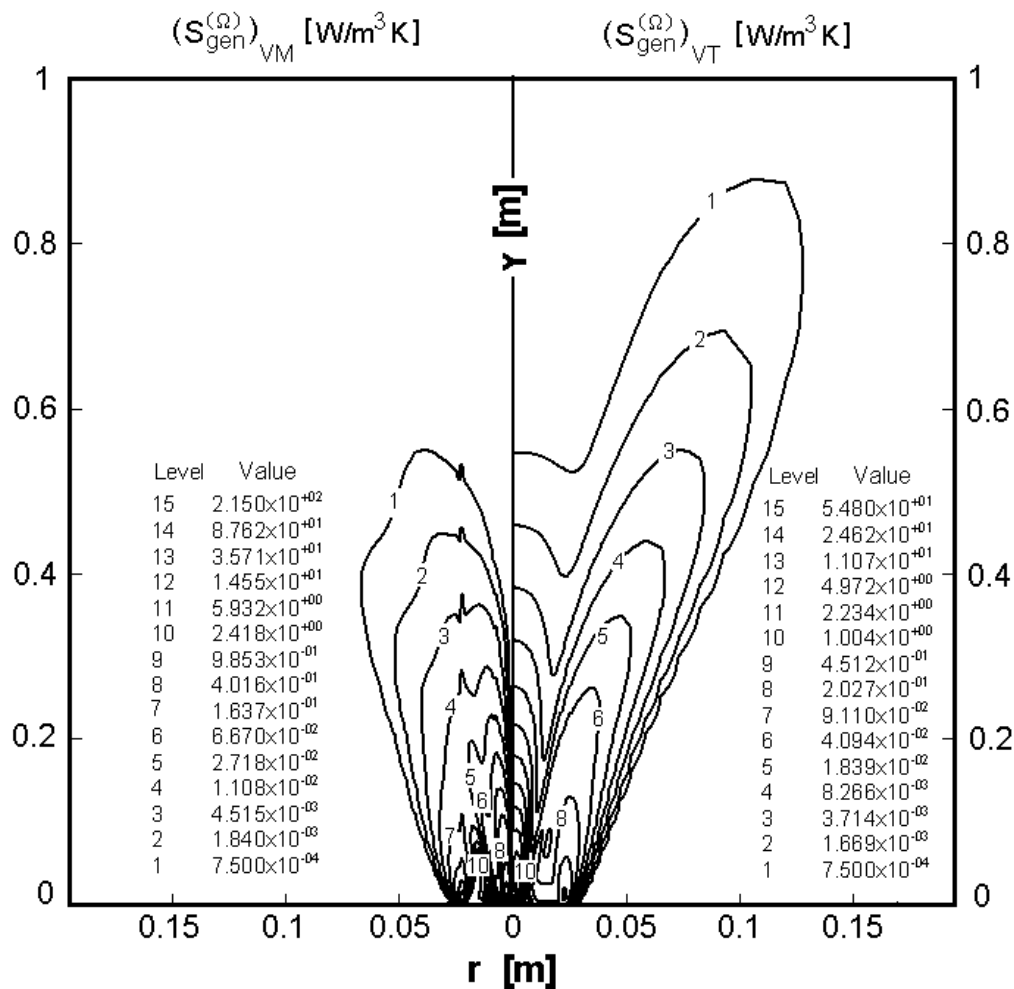


Figure 5a. Viscous mean motion and viscous turbulent volumetric irreversibilities

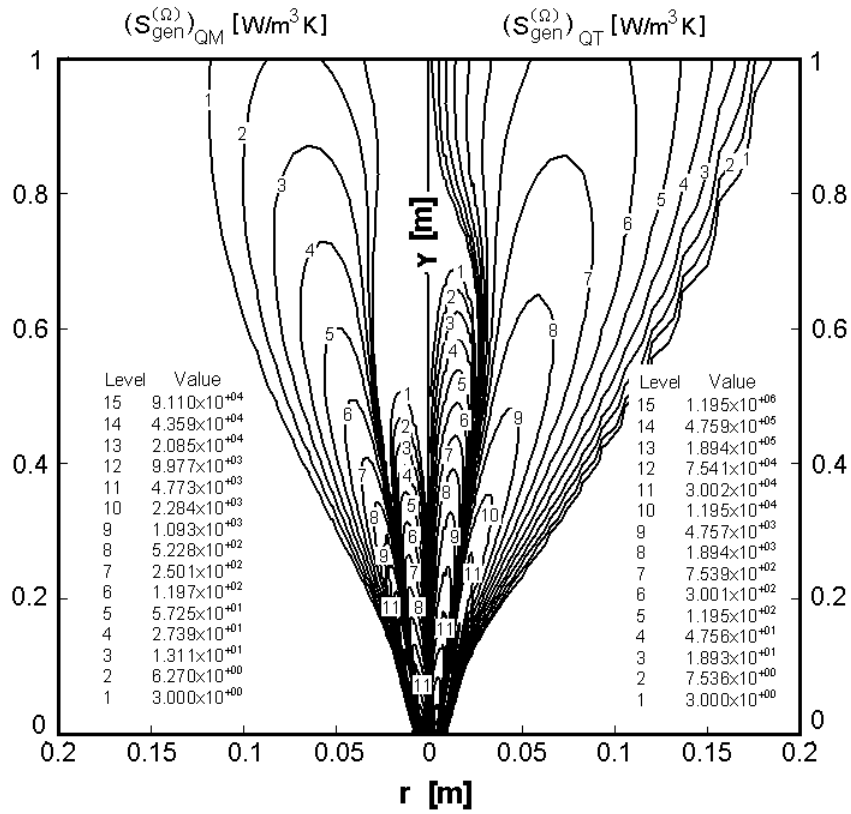


Figure 5b. Thermal mean motion and thermal turbulent volumetric irreversibilities

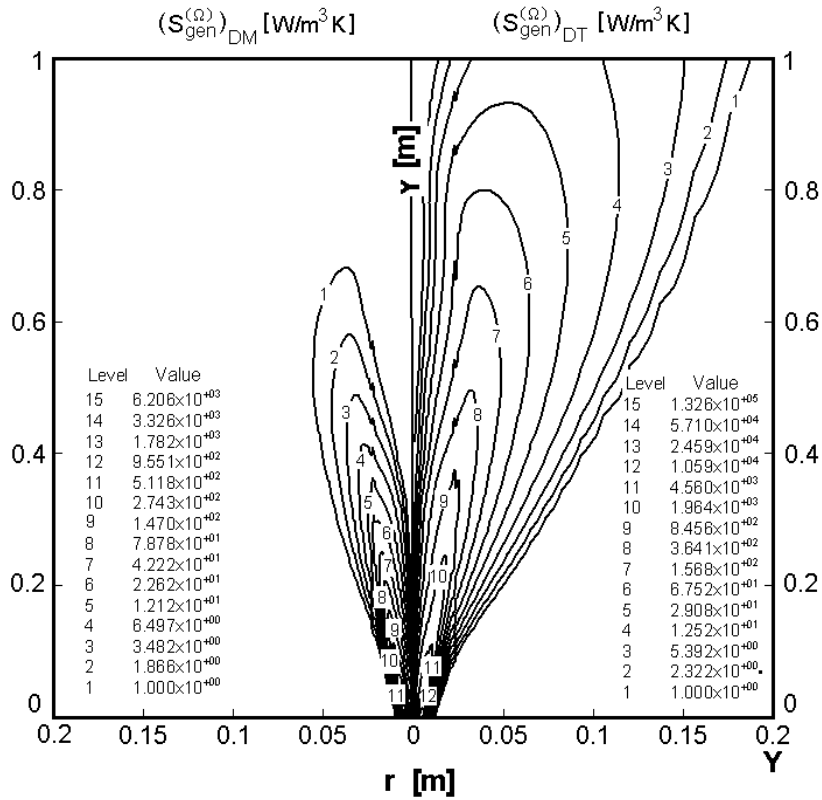


Figure 5c. Diffusion mean motion and diffusion turbulent volumetric irreversibilities

The left hand side of the above equation represents the mean entropy convection flux passing through boundaries and the right hand side stands for the mean entropy generation rate in the entire volume of the thermodynamic system. TABLE II presents the results of integration and the closing error of the entropy Eq. (59) for the two turbulence models used in this paper. It can be observed that the two turbulence models give similar results concerning both the entropy generation rate values and the closing error of the entropy Eq. (59), which is about of 6.5%. The most important conclusion revealed by this table is that the thermal turbulent and the chemical irreversibilities are responsible for 38% and 57% respectively, of the flame dissipation, while the diffusion irreversibilities destroy only 4% of the exergy. The relative importance of chemical dissipation could be a little over estimated because the eddy break-up model of Magnusen and Hjertager (1976) gives higher values for the mean reaction rate. On the other hand, these results may change in the case of recirculation and swirling diffusion flames, where the viscous and diffusion irreversibilities could increase.

3.3.2 Flame irreversibility simulation with assumed PDF approach for a conserved scalar

In this case the discretization of transport equations was carried out in a finite volume approach on a non-staggered, 50x50 nodes, non-uniform grid, following a semi-implicit numerical scheme. More details can be found in the work of Ferziger and Peric (Ferziger and Peric, 1995). Due to Launder's correction in the ϵ_K equation, the agreement between the numerical simulation and the experimental data (Isvoranu et al., 2000) is by far better than in the case of the multi-species model.

The distribution of irreversibility components does not differ very much from the previous case. Taking into account the model cannot make the separation between the mean motion part and the turbulent part of each irreversibility component; all the viscous, thermal and diffusion distributions of flame irreversibility have the carriage of corresponding turbulent irreversibilities that was previously presented. Some differences appear in the distribution of thermal and chemical irreversibility components, but they do not seriously alter the general aspect of variation. For this reason, the distributions of irreversibility components are not presented here, but under the form of ratios $(\bar{S}_{gen}^{(\Omega)})_K / (\bar{S}_{gen}^{(\Omega)})$, where subscript K stands for V, Q, D and CH can be found in (Isvoranu et al., 2000). Figure 6 displays only the spatial contours of volumetric entropy generation rate $\bar{S}_{gen}^{(\Omega)}$. It can be seen that the viscous irreversibilities border the spatial domain where the dissipations occur. In this domain, the relative importance of each mechanism is the changing function of the considered position. This importance can be estimated combining the results revealed by Figures 5 and 6. For example, in the fuel side at $y=0.4m$ high from the burner, about 75% of the total dissipation is due to the thermal irreversibilities (including the mean motion part with 1.5% and the turbulent part with 98.5%) and about 25% belong to the diffusion irreversibilities (mean motion part with 0.4% and 99.6% for the turbulent part). On the primary air side, the diffusion irreversibilities have a contribution of 5% to the total dissipation, the viscous ones only 2% and the thermal irreversibilities are responsible for the rest - 93%. As in the previous example, the turbulent parts of irreversibility components make the rule.

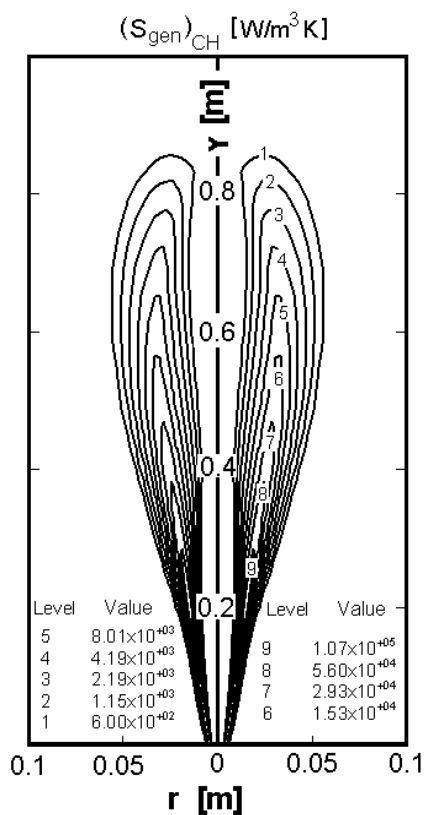


Figure 5d. Chemical mean motion volumetric irreversibility

TABLE II. INTEGRAL VALUES OF ENTROPY GENERATION RATES AND ENTROPY FLUX FOR TURBULENT FLAME (MULTI-SPECIES MODEL)

Model	$(\dot{S}_{gen})_{VM}$ [W/K]	$(\dot{S}_{gen})_{VT}$ [W/K]	$(\dot{S}_{gen})_{QM}$ [W/K]	$(\dot{S}_{gen})_{QT}$ [W/K]	$(\dot{S}_{gen})_{DM}$ [W/K]	$(\dot{S}_{gen})_{DT}$ [W/K]	$(\dot{S}_{gen})_{CH}$ [W/K]	\dot{S}_{gen} [W/K]	Entropy flux [W/K]	Error [%]
RNG K- ϵ_K	8.1×10^{-6}	0.0011	0.456	28.499	0.0283	2.896	41.967	73.847	69.397	6.4
Realiz. K- ϵ_K	8.9×10^{-6}	0.0019	0.508	31.752	0.0304	3.0486	39.824	75.16	70.792	6.1

Finally, the closing error of the entropy equation was computed. For the entropy flux, the Favre averaged specific entropy was determined with the same assumed PDF expression (41), because of its dependence mainly on mixture fraction. The result of flux integration (the left hand side of the entropy equation) was 92.04 W/K while the integration of volumetric entropy generation (the right hand side of the entropy equation) led to 77.2 W/K. As in the previous model, considering the entropy convection flux as a reference value, the relative error was about 16%. Comparing these values with those of TABLE II, the results show that the mean entropy flux is over-predicted. The main cause is probably the average procedure of specific entropy or the simplicity of the turbulence closure model.

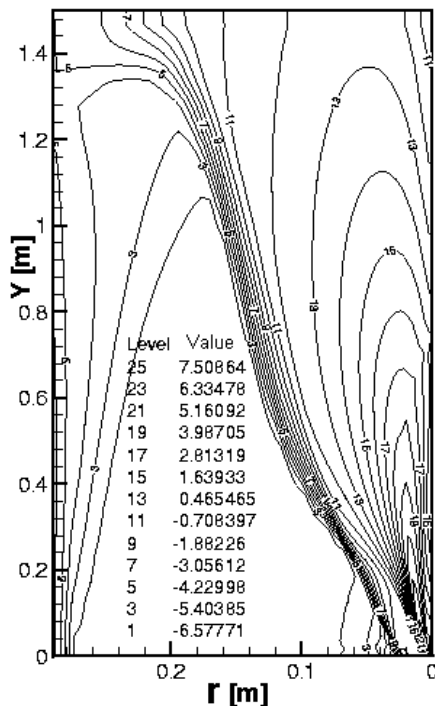


Figure 6. Distribution of $\log_{10}[(\dot{S}_{gen}^{(\Omega)})]$ computed with assumed PDF approach for a conserved scalar

4. Conclusion

In this paper we have investigated the irreversibility sources in both laminar and turbulent diffusion flames. The theoretical background of this investigation is done by the local balance equation of exergy (19), which relates the volumetric rate of exergy dissipations to the volumetric rate of entropy generation. This is nothing other than the local formulation of the well-known Gouy-Stodola theorem, linking it to the general concept of exergy dissipations from the second law formulation. It becomes obvious that one could wish these dissipations were the smallest possible, but in order to do this it is imperative to know what generates them and which is their structure and magnitude.

The second law analysis of laminar diffusion flame represents the first step in understanding the basic mechanism of dissipations in non-premixed combustion. The volumetric rate expression of entropy generation (26) shows that the viscous, thermal, diffusion and chemical components of the irreversibilities uncouple only under the hypothesis $|dP/P| \ll |dY_i/Y_i|$, which is valid for most of the engineering combustion applications. As an illustrative application, we performed a numerical entropy generation analysis for a laminar diffusion flame of co-flowing methane-air jets. The results point out that all the irreversibility components reach their maximum values at the flame front and, more importantly, only the thermal and chemical irreversibilities have significant contributions in the laminar reacting flow dissipations.

Most important for engineering applications are the turbulent diffusion flames. By its fluctuating field, the turbulence gives rise to new kind of irreversibilities, increasing the flame exergy dissipation. Although the multi-species approach does not prove great accuracy in simulating the reacting flow, it is able to separate the mean motion irreversibilities, which are the homologues of those ruling the laminar flame, from the proper irreversibilities of turbulence.

The numerical simulation of a turbulent co-flowing methane-air flame shows that the turbulent viscous, thermal and diffusion irreversibilities are considerably greater than those generated in the mean motion field. But as shown in TABLE II, among them, the thermal turbulent irreversibility, in addition to the mean chemical one dominate the exergy dissipation process occurring in the diffusion flames. Making the distinction between mean and fluctuating dissipations, this model emphasizes the two opposite effects of turbulence on combustion. On one side, the turbulence strongly augments the mixing and the reaction rate, allowing the flame stabilization at higher velocity than in laminar case, on the other side, it dramatically increases the dissipations.

The assumed PDF approach for a conserved scalar is more precise in describing the mean flow properties, so that its joint irreversibility model is more accurate in simulating the flame irreversibility distributions. Unfortunately, these distributions include both the mean motion and the turbulent parts of irreversibility components because the model does not have the ability to separate them. But it is known from the previous approach that the turbulent parts of irreversibilities prevail on the mean motion ones, and more importantly that the thermal turbulent components play a very important role in dissipations of flame exergy.

The knowledge of irreversibility component distributions, revealed by the two models presented in this work, can represent a powerful tool in order to alter some geometrical, inlet or boundary conditions, so that the global entropy generation rate, in other words the exergy loss, diminishes. Practically, this means to optimize the thermodynamic process which, in our case for example, would be reflected in obtaining the same maximum temperature but with a smaller entropy generation.

In spite of the differences, the two irreversibility models developed in this paper have a strong resemblance because each of them involves the dissipation rates of some fluctuating properties variance. We were able to set forth that these dissipations should be commonly related to the volumetric entropy generation rate so they get the theoretical foundation of the Second Law Analysis. Becoming strongly related to a physical meaning, all the dissipation rates appearing in the volumetric entropy generation rate expression, but the scalar dissipation rate with priority, did not remain mathematical artifices anymore.

The final remark deals with the necessity that any numerical discretization scheme or chemical mechanism should be investigated on

its consistency and robustness based on this Second Law approach, so that they do not produce locally a negative source of entropy. In addition, it can be emphasized that the precision of any numerical solution can be checked, by verifying the closing error of entropy transport equation.

Nomenclature

A	Chemical affinity
\mathbf{A}_k	Chemical specie
c_p	Specific heat at constant pressure
D	Single diffusion coefficient
D_{im}	Diffusion coefficient of i -specie in gaseous mixture
e	Specific internal energy
ex	Specific exergy
f	Probability density function
g	Specific free enthalpy
G	Free enthalpy
h	Specific enthalpy
H_F	Lower heating value
$H(x)$	Heaviside step function
K	Turbulent kinetic energy
K_θ	Fluctuating temperature variance
$K_\psi^{(i)}$	Fluctuating mass fraction variance of i -component
K_p	Equilibrium constant
Le	Lewis number
M	Molar mass
N	Number of mixture's species
P	Pressure
R_i	Specific mass constant of ideal gas
R_M	Universal constant of ideal gas
s	Specific entropy
Sc	Schmidt number
\dot{S}_{gen}	Entropy generation rate
T	Thermodynamic temperature
u_α	Velocity component
\dot{q}_α	Heat flux component in α direction
X_i	Molar fraction
Y_i	Mass fraction
Greek symbols	
α	Spatial direction of system coordinate
β	Coupling function
δ	Dirac function
$\delta_{\alpha\beta}$	Kronecker symbol
Δ	Dissipation term in conservative form of a transport equation
$\partial\Omega_C$	Boundaries of computational domain
ε_K	Dissipation rate of turbulent kinetic energy

ε_θ	Dissipation rate of fluctuating temperature variance
$\varepsilon_\psi^{(i)}$	Dissipation rate of fluctuating mass fraction variance of i -component
$\Phi_\alpha^{(i)}$	Diffusion flux component of i -specie in α direction
$g_\alpha^{(i)}$	Diffusion velocity component of i -specie in α direction
ν	Stoichiometric coefficient
μ	Viscosity
μ_i	Chemical potential of i -specie
$\mu_{M,i}$	Molar chemical potential of i -specie
Π	Production term in the conservative form of a transport equation
ρ	Density
ξ	Mixture fraction
χ	Scalar dissipation rate
χ_{st}	Stoichiometric scalar dissipation rate
ζ_{ch}	Chemical exergy
$\tau_{\beta\alpha}$	Stress tensor
τ	Time
ω	Reaction rate
Ω_C	Computational domain

Subscripts

.M	Mean
.T	Turbulent part
CH	Chemical part
D.	Diffusion
F	Fuel
M	Molar quantities
O	Oxydant
Q.	Thermal
T	Turbulent
V	Viscous
in	inert

Superscripts

$\overline{\varphi}$	Reynolds mean part of φ
$\widetilde{\varphi}$	Favre mean part of φ
φ''	Favre fluctuating part of φ
Ω	Volumetric
V	Viscous part
R	Reynolds part

References

Abou-Ellail, M. M., Salem, H., 1990, "A skewed PDF combustion model for jet diffusion flames", *Journal of Heat Transfer*, 112, pp. 1002-1007.

Bejan, A., 1983, *Entropy generation through fluid flow and heat*, John Wiley & Sons, New York.

Bejan, A., 1988, *Advanced Engineering Thermodynamics*, John Wiley & Sons, New York.

Burke, S. P., Schumann, T.E.W., 1928, "Diffusion flames". *Industrial and Engineering Chemistry*, 20, pp. 998-1004.

Elghobashi, S., 1977, "Studies in the prediction of turbulent diffusion flames", *Studies in Convection*, Vol. 2, B.E. Launder, Ed., Academic Press.

Ferziger, J. H., Peric, M., 1995, *Computational Methods for Fluid Dynamics*, Springer Verlag New York.

Fluent Inc.: "User's Guide vol II"

Isvoranu, D., 1999, "Contributions to chemical reacting flows optimization", Ph.D. Thesis, Polytechnic Univ. of Bucharest.

Isvoranu, D., Marinescu, M., Stanciu, D., "A Thermodynamic Approach towards Turbulent Diffusive Reactive Flows", *Proceedings of ECOS 2000*, pp. 313-324

Launder, B. E., Morse, A., Rodi, W., Spalding, D.B., 1972, "The prediction of free shear flows – A comparison of six turbulence models", Technical report, NASA SP – 311.

Libby, P., Williams, F. A., 1993, *Turbulent Reacting Flows*, Academic Press, New York.

Lockwood, F., C., 1977, "The Modeling of Turbulent Premixed and Diffusion Combustion in the Computation of Engineering Flows", *Combustion & Flame*, 29, pp 111-122.

Magnusen, B. F., Hjertager, B.,H., 1976, "On the Mathematical Model of Turbulent Combustion, with Special Emphasis on Soot Formation and Combustion", *16th Symp. On Combustion* (The Combustion Institute).

Peeters, T.W.J., 1995, "Numerical modeling of turbulent natural-gas diffusion flames", Ph.D. thesis, TU Delft.

Sanders, J.P.H., 1994, "Scalar transport and flamelet modeling in turbulent jet diffusion flames", Ph.D. thesis, Technische Universiteit Eindhoven.

Sciubba, E., 1994, "Entropy Generation Rates as a True Measure of Thermal and Viscous Losses in Thermochemical Components and Systems", *Workshop on Heat Transfer and Thermodynamics*, Bucharest.

Stanciu, D., 1999, "The Study of Viscous and Thermal Irreversibilities in Turbomachineries", Ph.D. Thesis, Polytechnic Univ. of Bucharest.

Stanciu, D., Isvoranu, D., Marinescu, M., 2000, "Entropy generation rates in flames", *Proceedings of ECOS 2000*, pp. 333-342

Stanciu, D., Isvoranu, D., Marinescu, M, 2000*,
“Second Law Analysis of the Turbulent Flat
Plate Boundary Layer”, *Int. Journal of Applied
Thermodynamics*, Vol. 3, No. 3, pp 99-104.

Shih, T.,H., Liou, W. W., Shabbir, A., Zhu, J.,
1995, “A New K- ϵ Eddy Viscosity Model for
High Reynolds Numbers Turbulent Flows-Model

Development and Validation”, *Computer Fluids*
24 (3).

Vilcu, R., 1988, *Irreversible Thermodynamics*,
Ed. Tehnica, Bucharest.

Williams, F.A., 1985, *Combustion Theory*,
Benjamin / Cummings Publishing Co., Menlo
Park, CA, second edition.